This article has been accepted for publication in a future issue of this journal, but has not been fully edited. Content may change prior to final publication. Citation information: DOI 10.1109/LRA.2018.2810958, IEEE Robotics and Automation Letters

The hBracelet: a wearable haptic device for the distributed mechanotactile stimulation of the upper limb

Leonardo Meli[1], Irfan Hussain[4], Mirko Aurilio[1], Monica Malvezzi[1], Marcia K. O'Malley[3], Domenico Prattichizzo[1,2]

***Abstract*—Haptic interfaces are mechatronic devices designed to render tactile sensations; although they are typically based on robotic manipulators external to the human body, recently, interesting wearable solutions have been presented. Towards a more realistic feeling of virtual and remote environment interactions, we propose a novel wearable skin stretch device for the upper limb called "hBracelet." It consists of two main parts coupled with a linear actuator. Each part contains two servo actuators that move a belt. The device is capable of providing distributed mechanotactile stimulation on the arm by controlling the tension and the distance of the two belts in contact with the skin. When the motors spin in opposite directions, the belt presses into the user's arm, while when they spin in the same direction, the belt applies a shear force to the skin. Moreover, the linear actuator exerts longitudinal cues on the arm by moving the two parts of the device. In this work we illustrate the mechanical structure, working principle, and control strategies of the proposed wearable haptic display. We also present a qualitative experiment in a teleoperation scenario as a case study to demonstrate the effectiveness of the proposed haptic interface and to show how a human can take advantage of multiple haptic stimuli provided at the same time and on the same body area. The results show that the device is capable of successfully providing information about forces acting at the remote site, thus improving telepresence.**

***Index Terms*—Haptics and Haptic Interfaces, Wearable Robots, Human-Centered Robotics, Telerobotics and Teleoperation**

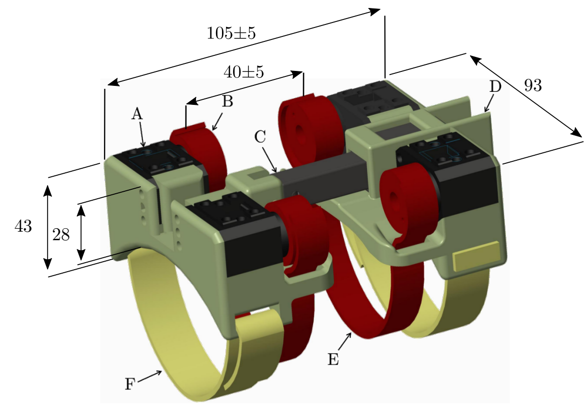

Fig. 1. The hBracelet consists of four servo motors and one linear actuator. The structural frame of the device is 3D printed. Dimensions of the prototype are expressed in millimeters. The total length of the device and the distance between the two belts depend on the linear actuator extension.

I. Introduction

THE complexity of the world around us is creating a demand for novel interfaces that will simplify and enhance the way we interact with the environment. The interaction that happens between the external environment and the user, mediated by a robotic manipulator, represents a typical teleoperation scenario, where the human user is the master and the artificial hand, manipulating external objects, is the slave [1]. In order to enable the user to have a more natural and realistic interaction during tele-operation tasks, it is important to provide the user with haptic sensations arising from such an interplay. In this respect, there is a variety of new wearable devices, called "wearables," that have been developed for this purpose. Wearables enable novel forms of communication, cooperation, and integration between humans and robots. Specifically, they enable the communication between the human wearer and the robotic device during the interaction with the environment they share. Different types of stimuli might be rendered on the human skin, such as information of pressure [2], and proprioceptive and directional cues [3], which are mainly related to skin stretch and deformation [4].

In this regard, we find *cutaneous technologies* very promising. Cutaneous cues are sensed by mechanoreceptors in the skin and they are useful to recognize the local properties of objects, e.g., shape, edges, embossings, and recessed features [5], [6]. The richness of information cutaneous receptors are able to detect, together with their broad distribution throughout the body, make the skin a perfect channel to communicate with the human user. Moreover, cutaneous haptic feedback represents an effective and elegant way to simplify the design

Manuscript received: September, 10, 2017; Revised December, 4, 2017; Accepted February, 10, 2018.

This paper was recommended for publication by Editor Yasuyoshi Yokokohji upon evaluation of the Associate Editor and Reviewers' comments. This work was supported by the European Union Seventh Framework Programme FP7/2007-2013 under grant agreement n°601165 of the project "WEARHAP" and from the European Union's Horizon 2020 Research and Innovation Programme under Grant Agreement n°688857 of the project "SoftPro".

[1]Dept. of Information Engineering, University of Siena, Via Roma 56, 53100 Siena, Italy. {leonardo.meli, mirko.aurilio, monica.malvezzi, domenico.prattichizzo}@unisi.it

[2]Dept. of Advanced Robotics, Istituto Italiano di Tecnologia, Via Morego 30, 16163 Genova, Italy.

[3]Dept. of Mechanical Engineering, Rice University, 6100 Main Street, Houston, TX, USA. omalleym@rice.edu

[4]Khalifa University Robotics Institute, Khalifa University of Science Technology and Research, Abu Dhabi, United Arab Emirates. irfan.hussain@kustar.ac.ae

Digital Object Identifier (DOI): see top of this page.

of haptic interfaces: the low activation threshold of skin receptors enables the design of small, lightweight, and inexpensive devices [7], [8], [9]. Cutaneous feedback also plays a key role in enhancing the performance and effectiveness of teleoperation systems [10], [11], as well as for the intuitive control of a prosthetic limb for transradial amputees [12]. Motamedi et al. [13] demonstrated that vibrotactile feedback is a viable replacement for visual attention during slippage and contact detection tasks performed by robotic manipulator. Thus, it might significantly improve the lives of upper-limb amputees.

Although there is a growing interest in wearable haptic displays, most are based on vibrotactile signals, or have limited force feedback modalities. Here, we present the hBracelet that is able to provide a multimodal mechanotactile stimulation at the same time and on the same body area, i.e., the user arm, through pressure and stretch cues related to normal, tangential, and longitudinal forces (see Fig. 1).

As a case study, we exploited the hBracelet in a telemanipulation scenario. The results show that the device is capable of informing the operator about different actions performed at the remote environment and allows one to successfully discern multiple haptic signals presented on the arm.

The rest of the paper is organized as it follows: Sec. II reports details on the device design and realization; Sec. III presents the mathematical formulation of the device; Sec. IV presents an application of the hBracelet in a teleoperation scenario and Sec. V the results and discussion of this qualitative experiment; finally, Sec. VI provides concluding remarks and perspectives of the work.

II. The hBracelet

To provide mechanotactile stimulation to the human upper limb we have designed the hBracelet, a wearable haptic interface whose CAD model is depicted in Fig. 1.

A. Hardware description

The hBracelet is composed of two main parts coupled with a Micro Linear Actuator L12-P (Actuonix, Canada) (C). The structural frame (D) of the device is symmetrical and 3D printed with polymeric ABS (Acrylonitrile Butadiene Styrene, ABSPlus, Stratasys, USA). Both parts of the device are composed of two Dynamixel XL-320 (Robotis, South Korea) actuators (A), two pulleys (B), a 3D printed thermoplastic polyurethane (Lulzbot, USA) belt (E), and a Velcro strap (F) for size adjusting. The distance between the front and rear belts can range between 35 mm and 45 mm. These values have been chosen to be sure the subject can distinguish between two independent haptic cues [14]. The hBracelet has a maximum dimension of (93x110x43) mm (see Fig. 1) and weighs 306 g. The maximum power consumptions of each Dynamixel motor (stall current 1.1 A @ 7.4 V) and of the Micro Linear Actuator (stall current 0.185 A @ 12 V) are 8.14 W and 2.22 W, respectively.

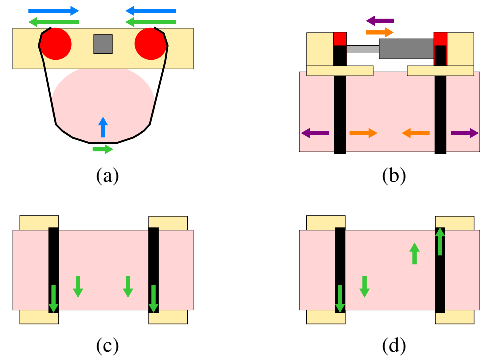

Fig. 2. Working principle of the hBracelet. (a) Squeezing (blue) and shear (green) forces due to the different pulleys spin direction. (b) Translational force (violet: opening; orange: closing) provided by the linear actuator. (c) Coherent shear force. (d) Opposite shear force.

B. Implementation

An OpenCM9.04-C controller (ROBOTIS Inc., USA) is connected with the computer and the Dynamixel motors through serial communication and TTL protocol, respectively. The linear actuator control (LAC) board, developed by Actuonix Motion Devices Inc. (USA), receives a digital signal (d_{LAC}) from the OpenCM9.04-C controller and in turn controls the motion of the linear actuator.

The linear actuator position d_{la} is computed according to the duty cycle of the input signal $d_{LAC} \in [0, 1]$ as

$$d_{la} = d_{LAC}\ M_{la}, \tag{1}$$

where $M_{la} = 2^{16}$ is the maximum actuator position.

Both the controller boards, the related electronic circuitry, and a battery pack are enclosed in a 3D printed box. While the linear actuator can be controlled only in position, the Dynamixel servo motors can be controlled both in velocity and position. In this application, we adopted velocity control for the "Auto-tuning procedure" (see Sec. II-C) and we took advantage of position control in all other cases to ensure better motion accuracy. The relationship between a single motor commanded angle $\Delta\theta$ and the corresponding belt length variation Δd is

$$\Delta d = r\Delta\theta, \tag{2}$$

where $r = 12.5\,\mathrm{mm}$ is the radius of the servo motor pulley and $\Delta\theta$ is expressed in radians. From now onwards, we will refer to the movement of motors in terms of rotation angles.

C. Auto-tuning procedure for the belts

An auto-tuning procedure has been implemented to set the home position of the belts, in order to optimally pre-tension the system for best perception. This is performed before any other action to make both belts in contact with the forearm. Indeed, at the beginning of each use the belts are fully open. The user wears the device and the auto-tuning procedure starts. Motors, rotating in opposite direction inward at the same speed, move the belts up. The contact between the arm and the belt is recognized when the load of a motor among the two exceeds an a priori set threshold; the reached motor position is set as the home position of this belt.

This article has been accepted for publication in a future issue of this journal, but has not been fully edited. Content may change prior to final publication. Citation information: DOI 10.1109/LRA.2018.2810958, IEEE Robotics and Automation Letters

TABLE I
HAPTIC FEEDBACK MODALITIES THE HBRACELET CAN PROVIDE. ACCORDING TO ACTUATOR SPECIFICATIONS, ACTUATION FORCE LIMITS ARE $0 < T_f < 16$N,$0 < T_r < 16$N, $0 < T_a < 20$N. THE MAXIMUM VALUES FOR THE TORQUES τ_f AND τ_r ARE EVALUATED CONSIDERING THE AVERAGE ARM DIAMETER $d_a = 75$mm.

T_1	T_2	T_3	T_4	T_a	Action Type and Range	Sketch	Real effect
0	0	0	0	τ_a	Longitudinal stretch $\max(A_f)=$ 20N	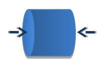	
τ_f	τ_f	0	0	0	Squeeze (front) $\max(N_f)=$ 32N	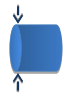	
0	0	τ_r	τ_r	0	Squeeze (rear) $\max(N_r)=$ 32N	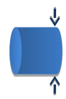	
τ_f	τ_f	τ_r	τ_r	0	Squeeze (whole arm)		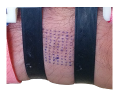
τ_f	$-\tau_f$	0	0	0	Shear (front) $\max(\tau_f)=$ 0.6Nm	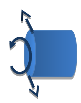	
0	0	τ_r	$-\tau_r$	0	Shear (rear) $\max(\tau_r)=$ 0.6Nm	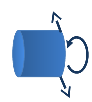	
τ_f	$-\tau_f$	τ_r	$-\tau_r$	0	Shear (coherent)	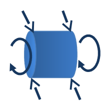	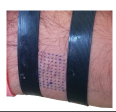
τ_f	$-\tau_f$	$-\tau_r$	τ_r	0	Shear (opposite)	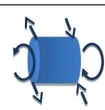	

D. Working Principle

Fig. 2 shows the four main types of haptic feedback the device can provide. In particular, when the pulleys of the motors which share the same belt spin in opposite directions (blue arrows), the belt applies a pressure on the user's arm generating a normal force (or release it, depending on the spin direction) as shown in Fig. 2a. When the motors spin in the same direction (green arrows), the belt applies a shear force to the skin. The linear actuator connecting the two bracelet parts is able to change their relative distance and therefore produce translational cues on the skin if no slippage occurs (see Fig. 2b). Since the hBracelet is equipped with two independently actuated belts, shear forces along different directions can generate different cutaneous sensations: when both the belts exert tangential force along the same direction, the device provides a shear sensation, either clockwise or counterclockwise (see Fig. 2c); when the two tangential forces have opposite direction the device provides a wringing effect, defined as opposite shear force in Fig. 2d.

Since each actuator of the hBracelet can be independently controlled, the squeezing action, or the shear force, can be provided by either one part of the device or both; the main hBracelet actuation types are summarized in Table I.

The limit of forces the device can apply are evaluated according to the actuators technical specifications. For the Dynamixel motors, we considered a reduced torque value of 0.2 Nm and not the maximum one, 0.39 Nm, since this value would lead to excessive forces on the arm that could be uncomfortable for the user. Furthermore, these limits take into account only actuators features, while the actual forces applied by the device will depend also on the arm compliance and friction properties. On the other hand, an evaluation of device performance including also these parameters would be dependent on the user specific anatomical parameters and therefore would be difficult to be evaluated and generalized.

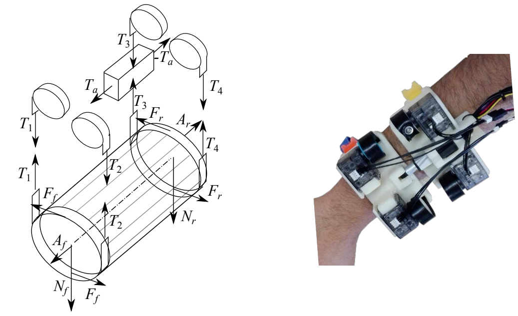

(a) (b)

Fig. 3. (a) Scheme of the forces acting on the arm and on the hBracelet when motors are actuated. (b) A subject wearing the hBracelet.

III. FORCE ANALYSIS

The scheme of the forces acting on the arm and on the hBracelet when the motors are actuated is shown in Fig. 3a, while Fig. 3b shows a subject wearing the hBracelet on the forearm. Let us indicate with T_1, T_2 tension values on the front pulleys, with T_3, T_4 tension values on the rear ones, and with T_a the linear actuator force.

The arm is subject to an overall action that can be represented as: i) a set of forces A_f, A_r acting in the longitudinal direction of the arm ("translation"); ii) a set of forces N_f, N_r acting on the normal (radial) direction of the arm ("squeeze"); iii) a set of tangential forces F_f, F_r ("shear"). An action, intended as any combination between a force and a torque exerted on the arm, can be obtained by suitably controlling the belts' tension and the linear actuator force. In the longitudinal direction we easily get

$$A_f = -A_r = T_a. \tag{3}$$

It is worth to underline that this expression is an approximation of the actual distribution of forces on the arm skin generated by the application of a force in the longitudinal direction. Indeed, such actions should also balance the bending moment due to the distance between actuator longitudinal main direction and arm longitudinal axis. However, in this application, since the structural force is filtered by the user's perception, we have assumed that the force in the longitudinal direction is dominant with respect to the distribution of tangential forces necessary to balance the bending moment, i.e., we have considered the longitudinal component of the force only. A more accurate estimation of the distribution of forces performed by the hBracelet is possible only considering also the compliance of arm tissues. Indeed, from the structural point of view the hBracelet fixed on the arm can be represented as an over-constrained structure; consequently, the complete equilibrium relationships can be solved only if the structural compliance of the system is known.

Considering the equilibrium of the hBracelet in the radial direction, the normal forces N_f, N_r on the front and rear sections can be evaluated as

$$N_f = T_1 + T_2, \quad N_r = T_3 + T_4. \tag{4}$$

When $T_1 \neq T_2$ and/or $T_3 \neq T_4$ bracelet forces generate a torque on the arm that is balanced by tangential forces created by the friction on the contact surface. Assuming, for the sake of simplicity, that the cross section of the arm can be represented as a cylinder with a radius R_f on the front section and R_r on the rear one, the torques generated by the difference in the hBracelet tensions are given by

$$\tau_f = R_f(T_1 - T_2), \quad \tau_r = R_r(T_3 - T_4) \tag{5}$$

and the corresponding tangential forces on the arm surface are given by

$$F_f = T_1 - T_2, \quad F_r = T_3 - T_4. \tag{6}$$

Considering as a first approximation a linear relationship between the actuators force and forces exerted on the arm, we can summarize the above introduced relationships as follows

$$\begin{bmatrix} A_f \\ A_r \\ N_f \\ N_r \\ \tau_f \\ \tau_r \\ F_f \\ F_r \end{bmatrix} = \begin{bmatrix} 0 & 0 & 0 & 0 & 1 \\ 0 & 0 & 0 & 0 & -1 \\ 1 & 1 & 0 & 0 & 0 \\ 0 & 0 & 1 & 1 & 0 \\ R_f & -R_f & 0 & 0 & 0 \\ 0 & 0 & R_r & -R_r & 0 \\ 1 & -1 & 0 & 0 & 0 \\ 0 & 0 & 1 & -1 & 0 \end{bmatrix} \begin{bmatrix} T_1 \\ T_2 \\ T_3 \\ T_4 \\ T_a \end{bmatrix}. \tag{7}$$

Such linear mapping can be used to generate composite actions on the arm, for example, if all the four actuators apply the same tension $T_1 = T_2 = T_3 = T_4$, the same normal force is applied both on the front and rear sections of the arm, leading to a distributed normal force (“squeeze whole arm”). If tangential torques with the same direction are applied again on both the front and rear sections, a distributed tangential force is perceived by the user (“coherent shear”). If tangential torques have different signs, e.g., $\tau_f > 0$ and $\tau_r < 0$ or vice versa, a wringing force is applied to the arm (“opposite shear”). Some of these actions are schematically shown in Table I.

IV. Human-robot applications

Human-Robot Interaction (HRI) is studied by researchers to understand and design robotic systems to use with or by humans. If the human and the robot are separated spatially or even temporally, we refer to these as remote interactions or teleoperation [15]. In order to demonstrate the effectiveness of the hBracelet, we conducted a qualitative experiment in a teleoperation scenario. The experiment had two main goals: i) understanding how humans can be able to discern multiple haptic information provided on the same body area, i.e., the forearm, at the same time; ii) finding an intuitive mapping between the haptic stimuli the hBracelet can yield and some information coming from the remote environment.

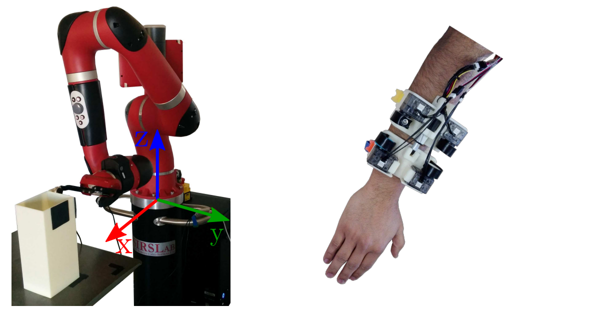

(a) Slave side (b) Master side

Fig. 4. Experimental setup. (a) Sawyer manipulator with two force sensors mounted on the robotic gripper. (b) hBracelet able to provide cutaneous cues on a subject’s forearm related to the information collected by the robot at a remote site.

Experimental setup: The proposed teleoperation system was composed of the hBracelet, detailed in Sec. II, a 7-DoF Sawyer manipulator (Rethink Robotics, US), and two OMD-20-SE-40N 3-DoF force sensors (Optoforce Ltd, HU) mounted on the robotic gripper. The object was a parallelepiped with dimensions of (80x95x20) mm placed on a specific position of the table in front of the robot (see Fig. 4). Many small spheres of different size and weight were inserted into an opening on top of the object. The total weight of the object ranged from 160 g (empty object) to 600 g (with all the spheres inside).

Implementation: Using the control strategies detailed in Secs. II and III, information collected by the robot on the slave side was fed back to the user on the master side through the hBracelet. The exchange of messages between all the different devices was managed by the ROS framework, an opensource Robot Operating System [16].

Participants: 10 right-handed subjects (7 males, 3 females, average age 26) participated in this qualitative study. Five of them had previous experience with haptic interfaces. None of the participants reported any deficiencies in their visual or haptic perception abilities. Participants were briefed about all the tasks and afterwards signed an informed consent, including the declaration of having no conflict of interest. All of them were able to give the consent autonomously. The participation in the experiment did not involve the processing of genetic information or personal data (e.g., health, sexual, lifestyle, ethnicity, political opinion, religious or philosophical conviction). Our organization does not require any IRB review for this case.

Methods: Participants were asked to control the robot on the slave side by keyboard inputs and without direct visual feedback of the remote environment. The possible behaviors of the robot are described by the finite-state machine shown

This article has been accepted for publication in a future issue of this journal, but has not been fully edited. Content may change prior to final publication. Citation information: DOI 10.1109/LRA.2018.2810958, IEEE Robotics and Automation Letters

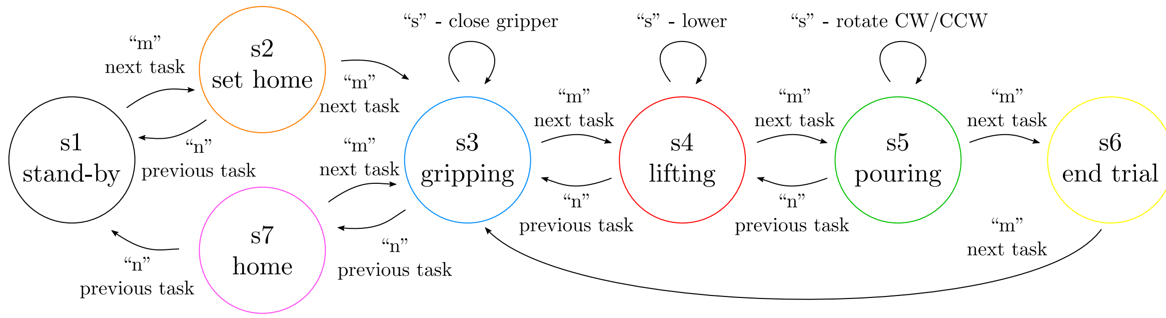

Fig. 5. The implemented finite state machine (FSM) to perform the experimental tasks.

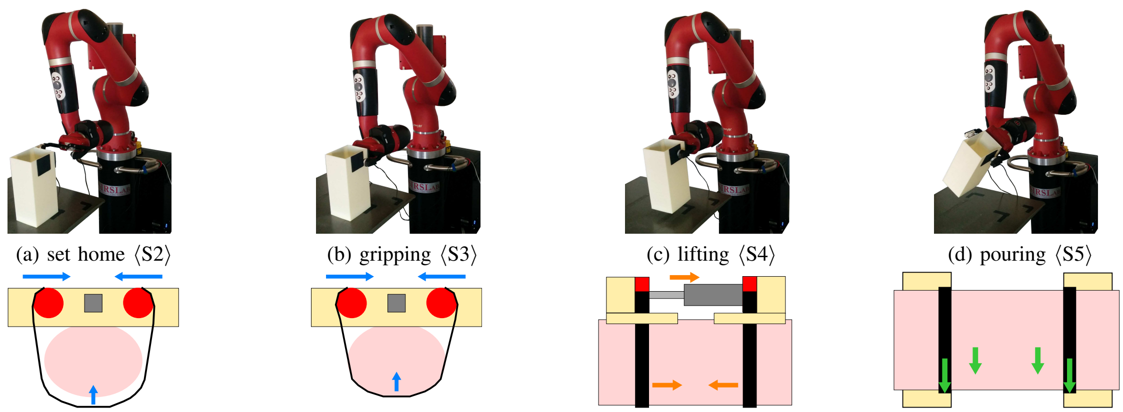

(a) set home ⟨S2⟩ (b) gripping ⟨S3⟩ (c) lifting ⟨S4⟩ (d) pouring ⟨S5⟩

Fig. 6. Sawyer manipulator positions (top) and corresponding hBracelet actions (bottom) during the main experimental tasks. The hBracelet actions refer only to the haptic feedback combination numbered as 1 in Table II as an example of use.

in Fig. 5. Each arrow, i.e., system event, is characterized by a keyboard key. Because of the lack of visual feedback, input commands are simplified: the operator uses "m" and "n" to change state and "s" to interact with the object. The type of interaction depends on the current state. Following all the states are described:

S1 - stand-by: hBracelet and Sawyer robotic arm are initialized; all connections between each controller and the computer are established. The belts of the hBracelet are released to easily don and doff;

S2 - set home: by means of the auto-tuning procedure that exploits motor torque readings (see Sec. II-C), the belts of the hBracelet come in contact with the forearm of the subject without compressing the skin; the robotic arm reaches the starting position (see Fig. 6a);

S3 - gripping: the connection between the robot and the hBracelet is enabled, i.e., the motors on the haptic display move accordingly to what happens at the remote site; the robot end-effector approaches the object, that, at end of the motion, will be exactly between the gripper clamps (see Fig. 6b); subjects are asked to close the gripper until they feel a stable squeezing force, i.e., the gripper is exerting the required force on the object and will no longer close. Subjects command the progressive closing of the gripper by typing "s" (each time "s" is typed, the reference closing distance of the gripper decreases by 7 mm);

S4 - lifting: the closing distance, i.e., the closing force, of the gripper is kept constant. Subjects are asked to lift up the object until they feel a constant sensation of weight. Subjects command the progressive lifting of the object by typing "s" (each time "s" is typed the end-effector position increases by 1 mm upwards). Once the object is no longer in contact with the table (see Fig. 6c), the force along z-axis (see Fig. 4a) is constant, i.e., the full object weight is perceived by the operator;

S5 - pouring: the robotic gripper automatically reaches a higher predetermined position (far enough from the table to do not hit it while rotating). This time, subjects are asked to rotate the object until they feel a change in its weight (see Fig. 6d). The preferred direction of pouring (randomly selected among clockwise (CW) and counterclockwise (CCW) in each trial) is indicated to user via the hBracelet skin stretch action.
Subjects command the progressive rotation of the object by typing "s" (each time "s" is typed the object is rotated about the x-axis, as defined in Fig. 4a, of 10°). When rotation reaches about 90°, the balls contained in the box begin to fall and the weight of the object changes;

S6 - end trial: when the subjects feel the change in weight, they can move to the last state completing the trial. A message appears on the screen in front of the subject to confirm the end of the trial, then by pressing "m" again, the object is placed back on the table;

This article has been accepted for publication in a future issue of this journal, but has not been fully edited. Content may change prior to final publication. Citation information: DOI 10.1109/LRA.2018.2810958, IEEE Robotics and Automation Letters

S7 - home: this state is reached from the gripping state by typing “n.” The robotic arm goes back to its starting position without setting a new home for the hBracelet, i.e., without repeating the auto-tuning procedure.

An experimental trial can be considered accomplished when, starting from S1, S6 (“end trial”) is visited.

Since subjects do not see what is happening at the remote site, each transition between subsequent states strongly depends on what subjects perceive on their forearm by means of the hBracelet interface. Headphones were worn to mask the noise of the motors. During the experiment, we mapped three pieces of information concerning the robot’s state to three different haptic stimuli:

- average gripping force sensed by the two force sensors mounted on the gripper → normal force of the hBracelet (“squeeze”);
- weight of the object (force along the z-axis in Fig. 4a) → longitudinal stretch/compression of the skin exerted through the linear actuator of the hBracelet (“translation”);
- torque about the x-axis estimated on the end-effector → tangential or wringing action of the hBracelet (“shear”).

We decided to use this specific mapping strategy because, in our opinion, this way the actions of the hBracelet recall as much as possible the real interaction with the remote object and subjects could intuitively understand what was happening at the remote site.

Besides the general mapping strategy detailed above, both the longitudinal motion of the linear actuator and the shear action can have some variants. Specifically, we can choose to set the initial position of the linear actuator either fully extended, or fully retracted. Similarly, we can choose to provide to the subject the sensation of torque using either the action defined as “shear opposite,” or the one defined as “shear coherent.” During this experimental evaluation the four combinations shown in Table II have been tested by each participant.

The intensity of all haptic stimuli was proportional to the measures gathered on the slave side. For the sake of simplicity and to be able to exactly control the motion of each motor, no matters the simultaneous feedback modalities considered, we used a position control. The force exerted by the robot during the grasping of the object ranged from 0 N to 10 N. This force range was mapped on the hBracelet motors reference position between 0° and 60°, i.e., skin indentation of the forearm ranging from 0 to 13 mm. This specific mapping was a priori decided following a pilot study in order to let the operators clearly perceive a squeezing force and keeping at the same time a large enough residual motors rotation to permit shear actions. The force exerted by the robot to hold the object (along the z-axis in Fig. 4a) varied from 0 N to 15 N, and it was mapped on the linear actuator extension range $0-10$ mm. It is worth noting that with a linear actuator extension of 0 mm the two main parts of the hBracelet were at a distance of 5 mm in order to prevent painful pinches for the users. The torque estimated by the robot ranged from -1 Nm and 1 Nm and was mapped on the hBracelet motors rotation from $-80°$ to $80°$ regarding the shear action. This range was a priori set using again pilot experiments: indeed, on average, this was the maximum feasible motion without exceeding motors position boundaries (motion due to the calibration and squeezing action need to be also considered). While it is easy to estimate skin indentation for the squeezing action, the skin stretch strongly depends on the friction between the skin and the device belts. In this case, a grasping action, corresponding to a skin indentation and an increase of friction, is fundamental to perceive a convincing shear action.

TABLE II
TASK FEATURES TO CUE MAPPINGS AND MEAN NUMBER OF MISSES DURING THE EXPERIMENT (N=10).

				# misses per task		
	object weight	**gripping force**	**torque**	S3	S4	S5
1	transl. inward	squeeze	shear coherent	0	1	0
2	transl. outward	squeeze	shear coherent	0	0	0
3	transl. inward	squeeze	shear opposite	1	2	0
4	transl. outward	squeeze	shear opposite	0	1	0
			tot. # misses	1	4	0

All the rotation angles are measured with respect to the motors home position set during the auto-tuning procedure detailed in Sec. II-C.

Evaluation: In order to evaluate the performance of the considered feedback modalities, we recorded throughout the experiment i) the gripping force exerted by the slave robot; ii) the force along the z-axis in Fig. 4a (estimated weight of the object when lifted); iii) the estimation of the torque varying because of the pouring action and the motion of the spheres inside the grasped object; iv) the timestamp of any keyboard input. Moreover, after completing the test, the participants were asked to fill out a questionnaire which sought to evaluate the value of transmitting robot state information to the user via the hBracelet. In the first part subjects had to provide their demographic information, such as age and gender; in the second part they had to evaluate each feedback modality according to a 11-point scale, in particular subjects had to choose a maximum score (10) if they completely agreed and a minimum score (0) if they completely disagreed. Participants were also asked to select the haptic combination among the four proposed, that guaranteed the best perception of what was happening at the remote site. Finally, subjects rated their experience evaluating the level of comfort of the device from 0 (“very low”) to 10 (“very high”).

V. RESULTS AND DISCUSSION

Fig. 7 shows how a representative subject reacts to the haptic feedback provided by the hBracelet during the three main experimental tasks, characterized by states S3, S4, S5 of the FSM depicted in Fig. 5. In Fig. 7a the solid red line shows the mean of the gripping force along the y-axis (see Fig. 4) measured by the two force sensors placed on the end-effector. Such a force is provided through the squeezing action on the subject’s forearm by means of the hBracelet. The dashed vertical orange lines represent each moment the subject presses the key “s” on the keyboard, i.e., reducing the

This article has been accepted for publication in a future issue of this journal, but has not been fully edited. Content may change prior to final publication. Citation information: DOI 10.1109/LRA.2018.2810958, IEEE Robotics and Automation Letters

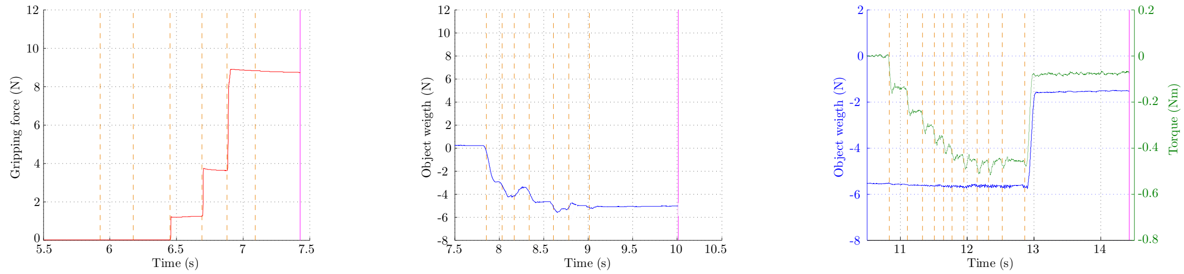

(a) gripping ⟨S3⟩ (b) lifting ⟨S4⟩ (c) pouring ⟨S5⟩

Fig. 7. Data recorded during the three most critical experimental phases, namely S3, S4, and S5, during an experiment carried out by a representative subject. The dashed vertical orange lines represent each moment the user presses the key "s" to interact with the object, i.e., reducing the reference closing distance in S3, increasing the end-effector position upwards in S4, increasing the object rotation in S5. The solid vertical magenta lines represent each moment the user presses the key "m" to change task, i.e., state of the FSM. The solid red line in (a) shows the measured gripping force, the solid blue lines in (b) and (c) the estimated force along the z-axis, and the dotted green line in (c) the torque about the x-axis estimated by the robot.

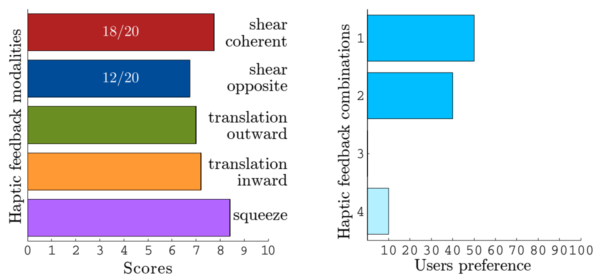

(a) (b)

Fig. 8. Questionnaire replies. (a) Means of evaluation of each feedback modality (according to a 11-point scale). On the top two bars the number of times users guessed the direction of rotation of the grasped object using that feedback modality. (b) Subjects preference (%) about the best haptic combination provided by the hBracelet among the four listed in Table II.

referencer closing distance of the gripper. The solid vertical magenta line shows when the subject presses "m" to change the task, i.e., moving to the next FSM state. Even though there is no visual feedback of the robot workspace, the subject is able to detect when the gripping force no longer increases: indeed, there are no extra dashed vertical orange lines since the force becomes constant. Something similar happens in Fig. 7b. This time the solid blue line indicates the force along the z-axis. Again, since the force becomes almost constant, there are no dashed vertical orange lines before the solid vertical magenta line, showing that the subject understands when the object is no longer in contact with the table by means of the longitudinal skin stretch. Finally, in Fig. 7c, the solid blue line represents again the force along the z-axis and the dotted green line shows the torque measured by the robotic end-effector about the x-axis. When the balls contained inside the object move and start to fall down the subjects perceives a two-fold change in the haptic feedback concerning both the longitudinal skin stretch and the shear action. Again the representative subject is perfectly able to detect such a change at the remote site and pressing "m" can move to S6 of the FSM completing the experimental trial. Let us define a metric as "number of misses": every time the subject presses the key "s" when she/he was supposed to move to the next task, i.e., the subject does not properly perceive the state of the remote robot, this counter is increased by one. On the right side of Table II the number of misses divided per task to accomplish and per feedback combination are shown. Although all the values are low, no misses occurred for the pouring task (S5). This might be due to the fact that the subjects were perceiving both the skin stretch and the shear action, thus multiple cues to understand what was happening at the remote site. Moreover, as it is shown in Fig. 7c, all the balls fall down at the same moment, causing a significant change in the haptic feedback in a short time. In task S4 subjects made the larger number of mistakes. Even though the haptic stimulus perceived was part of the one in which subjects did no misses (S5), this time, as it shown in Fig. 7b, the estimated weight slowly changed while lifting the object, making it more difficult to understand when it became constant. About the gripping task (S3), only one miss occurred over the total 40 trials. It is worth highlighting that among all the subjects, no one made more that a single miss in a trial.

Fig. 8a shows the mean of the evaluations given by the participants through a questionnaire for each feedback modality in order to understand which was the preferred modality for each robot state, i.e., the haptic signals that provided the clearest image of what was happening on the slave side. Apart the evaluation of each feedback modality, i.e., "shear opposite," "shear coherent," "translation outward," "translation inward," and "squeeze," participants were asked to choose the best haptic combination among the ones summarized on the left part of Table II, that gave them the feeling of performing better throughout the experiment. Subjects preference is reported in Fig. 8b in which on the y-axis haptic feedback combinations, numbered as in Table II, are shown, while the x-axis represents the percentage of people who preferred that specific combination compared to the others. A single response was accepted for each user. 50% of subjects chose the combination of "translation inward," "squeeze" and "shear coherent"; 40% of subjects chose the combination of "translation outward," "squeeze" and "shear coherent"; and 10% of subjects chose the combination of "translation outward", "squeeze" and "shear opposite".

The results obtained show that the squeeze action exerts a clear stimulus, useful in informing the subject about the force the object is grasped with. Furthermore, there seems to be no difference between the two modalities of translation, in fact

This article has been accepted for publication in a future issue of this journal, but has not been fully edited. Content may change prior to final publication. Citation information: DOI 10.1109/LRA.2018.2810958, IEEE Robotics and Automation Letters

they have reached a very similar number of preferences. The most interesting result concerns the shear action; in particular 90% of participants preferred "shear coherent" instead of "shear opposite." This result was not as evident in Fig. 8a, even though the score for the "shear coherent" was more than 1 point higher. It is worth pointing out that the use of the "shear coherent" modality led to a significantly better understanding of the rotation direction of the objects: as shown on the top two bars of Fig. 8a, the number of times the users guessed the direction of rotation of the grasped object is 18 for the "shear coherent" and 12 for the "shear opposite," over a total of 20 trials. The total number of trials is 20 because the "shear coherent" action was present in two feedback combinations, the first and the second (see Table II). The same for the "shear opposite" actions that was present in both the third and fourth combinations.

Finally, the comfort of the system received an average rating of 6.8 out of 10. Although this rating is more than fair, it shows the need to further improve the device ergonomics. According to the collected feedback modality preference of the subjects, the device designed can be revised to reduce the total weight and increase its level of comfort, thus its wearability.

VI. Conclusion and Future Work

This work presents a novel wearable force feedback haptic device for the upper limb which we called "hBracelet." It is able to provide the distributed mechanotactile stimulation on the user arm skin by means of pressure and stretch cues related to normal, tangential, and longitudinal forces. We described the mechanical structure, working principle, mathematical formulation, and control of the proposed device.

In order to evaluate the performance of the hBracelet, we conducted a qualitative experiment in a teleoperation scenario where the hBracelet was worn by a human and a robot was in remote communication via the device. This experiment allowed us to characterize the haptic feedback of the developed device. Furthermore, it provided information to understand how humans can be able to discern multiple haptic cues provided on the same body area, i.e., the forearm, at the same time and also to find an intuitive mapping between the haptic stimuli the hBracelet can yield and some information coming from a remote environment. The results show that the device is capable of informing about the forces acting at the remote site while performing a grasping and pouring task, hence improving the performance of the teleoperation system. In the future, we plan to run a more extensive evaluation, enrolling more human subjects and rigorously assessing the value of distributed mechanotactile stimulation. Work is ongoing to analyze each feedback modality performance quantitatively. Moreover, we aim to improve the wearabiltiy and ergonomics of the device by reducing the number of actuators, or selecting more compact form-factor ones. It is worth to underline that this version of the hBracelet has been designed with very powerful actuators to overcome any mechanical uncertainty and guarantee several clear independent haptic cues. In general, the qualitative study presented in this work represents a valuable contribution for further design choices and improvements of the hBracelet. Psychophysical studies will also be crucial in deciding how to change the device still keeping satisfying, distinct, and effective haptic cues. Finally, a comparison evaluation with a device capable of providing direction cues by means of vibrotactile patterns is of interest.

References

[1] J. Vertut, *Teleoperation and robotics: applications and technology*, vol. 3. Springer Science & Business Media, 2013.

[2] P. E. Patterson and J. A. Katz, "Design and evaluation of a sensory feedback system that provides grasping pressure in a myoelectric hand," *J Rehabil Res Dev*, vol. 29, no. 1, pp. 1–8, 1992.

[3] A. Bicchi, E. P. Scilingo, E. Ricciardi, and P. Pietrini, "Tactile flow explains haptic counterparts of common visual illusions," *Brain research bulletin*, vol. 75, no. 6, pp. 737–741, 2008.

[4] S. Casini, M. Morvidoni, M. Bianchi, M. Catalano, G. Grioli, and A. Bicchi, "Design and realization of the cuff-clenching upper-limb force feedback wearable device for distributed mechano-tactile stimulation of normal and tangential skin forces," in *Proc. IEEE/RSJ Int. Conf. on Intelligent Robots and Systems*, pp. 1186–1193, 2015.

[5] I. Birznieks, P. Jenmalm, A. W. Goodwin, and R. S. Johansson, "Encoding of direction of fingertip forces by human tactile afferents," *The Journal of Neuroscience*, vol. 21, no. 20, pp. 8222–8237, 2001.

[6] K. O. Johnson, "The roles and functions of cutaneous mechanoreceptors," *Current opinion in neurobiology*, vol. 11, no. 4, pp. 455–461, 2001.

[7] D. Prattichizzo, F. Chinello, C. Pacchierotti, and M. Malvezzi, "Towards wearability in fingertip haptics: a 3-dof wearable device for cutaneous force feedback," *IEEE Transactions on Haptics*, vol. 6, no. 4, pp. 506–516, 2013.

[8] K. Minamizawa, S. Fukamachi, H. Kajimoto, N. Kawakami, and S. Tachi, "Gravity grabber: wearable haptic display to present virtual mass sensation," in *Proc. ACM Special Interest Group on Computer Graphics and Interactive Techniques Conference*, pp. 8–es, 2007.

[9] C. Pacchierotti, G. Salvietti, I. Hussain, L. Meli, and D. Prattichizzo, "The hring: A wearable haptic device to avoid occlusions in hand tracking," in *Proc. IEEE Haptics Symposium*, pp. 134–139, 2016.

[10] K. J. Kuchenbecker, D. Ferguson, M. Kutzer, M. Moses, and A. M. Okamura, "The touch thimble: Providing fingertip contact feedback during point-force haptic interaction," in *Proc. Symposium on Haptic interfaces for virtual environment and teleoperator systems*, pp. 239–246, 2008.

[11] C. Pacchierotti, L. Meli, F. Chinello, M. Malvezzi, and D. Prattichizzo, "Cutaneous haptic feedback to ensure the stability of robotic teleoperation systems," *The International Journal of Robotics Research*, vol. 34, no. 14, pp. 1773–1787, 2015.

[12] C. Antfolk, M. D'Alonzo, M. Controzzi, G. Lundborg, B. Rosén, F. Sebelius, and C. Cipriani, "Artificial redirection of sensation from prosthetic fingers to the phantom hand map on transradial amputees: vibrotactile versus mechanotactile sensory feedback," *IEEE transactions on neural systems and rehabilitation engineering*, vol. 21, no. 1, pp. 112–120, 2013.

[13] M. R. Motamedi, J.-B. Chossat, J.-P. Roberge, and V. Duchaine, "Haptic feedback for improved robotic arm control during simple grasp, slippage, and contact detection tasks," in *Proc. IEEE Int. Conf. on Robotics and Automation*, pp. 4894–4900, 2016.

[14] K. Myles and M. S. Binseel, "The tactile modality: a review of tactile sensitivity and human tactile interfaces," tech. rep., Army research lab Aberdeen proving ground MD human research and engineering directorate, 2007.

[15] M. A. Goodrich and A. C. Schultz, "Human-robot interaction: a survey," *Foundations and trends in human-computer interaction*, vol. 1, no. 3, pp. 203–275, 2007.

[16] M. Quigley, K. Conley, B. Gerkey, J. Faust, T. Foote, J. Leibs, R. Wheeler, and A. Y. Ng, "Ros: an open-source robot operating system," in *ICRA workshop on open source software*, vol. 3, p. 5, 2009.